

Establishing Isotopic Measurement Capabilities using Laser-Induced Breakdown Spectroscopy for the Molten Salt Reactor Campaign



Hunter B. Andrews
Joanna McFarlane

September 2023



DOCUMENT AVAILABILITY

Reports produced after January 1, 1996, are generally available free via OSTI.GOV.

Website www.osti.gov

Reports produced before January 1, 1996, may be purchased by members of the public from the following source:

National Technical Information Service
5285 Port Royal Road
Springfield, VA 22161
Telephone 703-605-6000 (1-800-553-6847)
TDD 703-487-4639
Fax 703-605-6900
E-mail info@ntis.gov
Website <http://classic.ntis.gov/>

Reports are available to US Department of Energy (DOE) employees, DOE contractors, Energy Technology Data Exchange representatives, and International Nuclear Information System representatives from the following source:

Office of Scientific and Technical Information
PO Box 62
Oak Ridge, TN 37831
Telephone 865-576-8401
Fax 865-576-5728
E-mail reports@osti.gov
Website <https://www.osti.gov/>

This report was prepared as an account of work sponsored by an agency of the United States Government. Neither the United States Government nor any agency thereof, nor any of their employees, makes any warranty, express or implied, or assumes any legal liability or responsibility for the accuracy, completeness, or usefulness of any information, apparatus, product, or process disclosed, or represents that its use would not infringe privately owned rights. Reference herein to any specific commercial product, process, or service by trade name, trademark, manufacturer, or otherwise, does not necessarily constitute or imply its endorsement, recommendation, or favoring by the United States Government or any agency thereof. The views and opinions of authors expressed herein do not necessarily state or reflect those of the United States Government or any agency thereof.

Radioisotope Science and Technology Division

**ESTABLISHING ISOTOPIC MEASUREMENT CAPABILITIES USING LASER-
INDUCED BREAKDOWN SPECTROSCOPY FOR THE MOLTEN SALT REACTOR
CAMPAIGN**

Hunter B. Andrews
Joanna McFarlane

September 2023

Prepared by
OAK RIDGE NATIONAL LABORATORY
Oak Ridge, TN 37831
managed by
UT-BATTELLE LLC
for the
US DEPARTMENT OF ENERGY
under contract DE-AC05-00OR22725

CONTENTS

LIST OF FIGURES	iv
ABSTRACT.....	1
1. INTRODUCTION	1
2. EXPERIMENTAL.....	1
3. RESULTS AND DISCUSSION.....	3
3.1 MEASUREMENTS ON FILTER SUBSTRATES.....	3
3.2 MEASUREMENTS ON AEROSOLS.....	6
3.3 COMPARISON OF FILTER AND AEROSOL CALIBRATION MODELS	8
4. SUMMARY AND FUTURE WORK	9
5. ACKNOWLEDGMENTS	9
6. REFERENCES	10

LIST OF FIGURES

Figure 1. Notional diagram of LIBS H isotope measurements performed on glass fiber filters.	2
Figure 2. LIBS plasma being formed at the tip of the injector exit.	3
Figure 3. Single-shot spectra versus 64-shot average spectrum of 0% D ₂ O used to better resolve peak center.	4
Figure 4. (a) Hydrogen emission line versus D/H ratio ranging from 0% to 100% D ₂ O and (b) the test sample shown with the dashed black line consists of 3,000 ppm Gd in 100% D ₂ O.	5
Figure 5. Parity plot comparing known versus predicted values of D ₂ O using (a) PCR and (b) PLSR. The closer the marker to the 1:1 line, the more accurate the prediction.	6
Figure 6. Parity plot comparing known versus predicted values of D ₂ O using (a) PCR and (b) PLSR. The closer the marker to the 1:1 line, the more accurate the prediction.	7
Figure 7. PCR model trained on filter data used to predict aerosol samples.	8
Figure 8. PCR model trained on filter data used to predict aerosol samples after the additional mean centering preprocessing step.	9

ABSTRACT

Proof-of-principle H isotope ratios of aqueous aerosol systems and liquid droplets on filter paper have been measured using laser-induced breakdown spectroscopy (LIBS) with root mean square error of prediction values down to 1.9%. Molten salt reactors (MSRs) will consist of a complex chemical and radiological system consistently producing new fission products as the reactor operates. Some of these fission products and/or their daughter species will leave the salt in the reactor off-gas. Monitoring the composition of the off-gas, as well as the salt itself, is important for monitoring reactor performance, including burnup, corrosion, and the concentration of impurities. Tritium is of concern for MSRs because it will be produced from the irradiation of key salt constituents, including Li and Be. LIBS offers an avenue for in situ salt and off-gas monitoring by firing a laser onto or into the sample stream to generate a plasma. The plasma light can be monitored to measure an elemental fingerprint of the sample. Extending this analysis to include isotopic ratios offers a critical expansion of the in situ monitoring capabilities being developed. This study demonstrates the expansion of Oak Ridge National Laboratory's LIBS capabilities to monitor isotopes and shows how simple calibrations may provide rapid semiquantitative models.

1. INTRODUCTION

Molten salt reactors (MSRs) are complex systems with system-wide chemistry challenges differing from their solid-fueled, light-water reactor cousins. MSRs consist of a primary reactor loop containing either fluoride or chloride salt mixtures with dissolved fissile fuel. This unclad fuel will fission in the reactor, producing heat and fission products, some of which will readily evolve from the salt. Other species may be produced through decay or subsequent neutron absorbance, leading to further species, which could either be volatile or migrate into the reactor head space through aerosolization. An off-gas system is critical to the operation of MSRs, serving to remove these products, properly confine them, and maintain an inert environment for the fuel salt.¹

In recent years, several studies have been performed in an organized effort to establish off-gas treatment components and online monitoring capabilities. Briefly, proof-of-principal, real-time monitoring of aerosols and noble gases has been performed using laser-induced breakdown spectroscopy (LIBS).²⁻⁵ LIBS has been used to evaluate the performance of metal-organic frameworks for selectively capturing Xe as a demonstration of in situ monitoring off-gas components.⁶ Raman spectroscopy systems have been developed to monitor iodine species.⁷ Raman and ultraviolet-visible absorbance spectroscopies have been used in tandem to monitor salt and gas phase changes simultaneously.⁸ The next steps in this effort involve deploying initial sensors on molten salt loops to perform larger-scale testing and to further expand the capabilities of these sensors to monitor additional species.

Hydrogen, being the lightest element in the periodic table, experiences the largest relative mass difference between its isotopes: protium, deuterium, and tritium. This difference, in turn, means the H-alpha Balmer line at 656 nm in a LIBS spectrum experiences a significant isotopic peak shift.⁹ Tritium is of significant interest in MSRs because it will be continuously produced during operation, and it is especially permeable.¹ These points indicate that H isotopes are an ideal initial system to initiate isotopic measurements via LIBS.

2. EXPERIMENTAL

Various ratios of D₂O (99.99%, Sigma Aldrich) and deionized H₂O (18 MΩ/cm) were loaded into sample vials using a 20 μL pipette. The vials were shaken vigorously to ensure the liquids mixed. Samples ranging from 0% to 99.9% D₂O in increments of 10% were prepared, resulting in 11 samples. For initial

tests, 10 μL of each sample were pipetted onto a 5 mm punch-out of a Whatman glass fiber filter affixed to a glass microscope slide using double-sided carbon tape. The 10 μL of sample was selected because it fully saturated the filter without excess liquid. The samples were immediately placed into the LIBS system for testing before any liquid could evaporate.

The LIBS system used was a LIBS-8 module from Applied Photonics with a 1,064 nm Nd:YAG laser operating at 150 mJ/shot at 10 Hz. The system allowed for the sample and optical pathway to be purged with high-purity Ar (AirGas, 99.999%) to prevent detecting atmospheric H in H_2O . The laser was focused onto the sample surface to a 100 μm diameter spot. The plasma light was collected at a slight angle from the incident laser pulse and measured using an echelle-type spectrometer (Mechelle 5000, Andor) affixed with an intensified charge-coupled device (iStar intensified charge-coupled device [ICCD], Andor) as the detector. The spectrometer ($\lambda/\Delta\lambda = 5000$) was wavelength-calibrated prior to testing using a HgAr lamp (SL2, StellarNet). The spectrometer delay and width were set to 2 and 50 μs , respectively, and a 4,000 gain was used to intensify the measured spectra. For each sample, an 8×8 shot pattern was performed, providing 64 spectra per sample. A diagram of this experiment is shown in Figure 1.

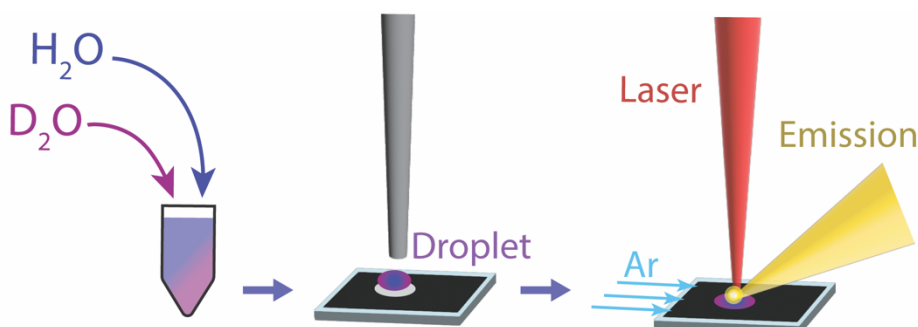


Figure 1. Notional diagram of LIBS H isotope measurements performed on glass fiber filters.

Aerosol measurements were performed using the same LIBS system. Aerosols were generated by siphoning sample from the sample vials using a peristaltic pump into a concentric nebulizer, along with high-purity Ar (AirGas, Ultra High Purity). The produced aerosols were then sent into a cyclone spray chamber, where larger droplets were removed from the stream. The larger droplets that accumulated in the spray chamber were constantly collected and removed using the same peristaltic pump in the reverse direction. The mist of fine aerosols was passed through an injector with its exit situated close to the LIBS plasma. A picture of the plasma forming at the tip of the injector is shown in Figure 2. The same spectrometer settings were used in the aerosol tests; however, only a subset of the ICCD chip was used to increase the spectrometer's maximum frame rate above 10 Hz. This increase allowed data to be collected far more rapidly than the 4 Hz limitation when using the entire echelle image. A total of 1,000 shots were collected for each sample, and air was pumped through the system between runs to purge the aerosol system. Typically, 4 mL of sample were used for each run, including 2 min of aerosol production to flush the system, ensuring no sample crossover.

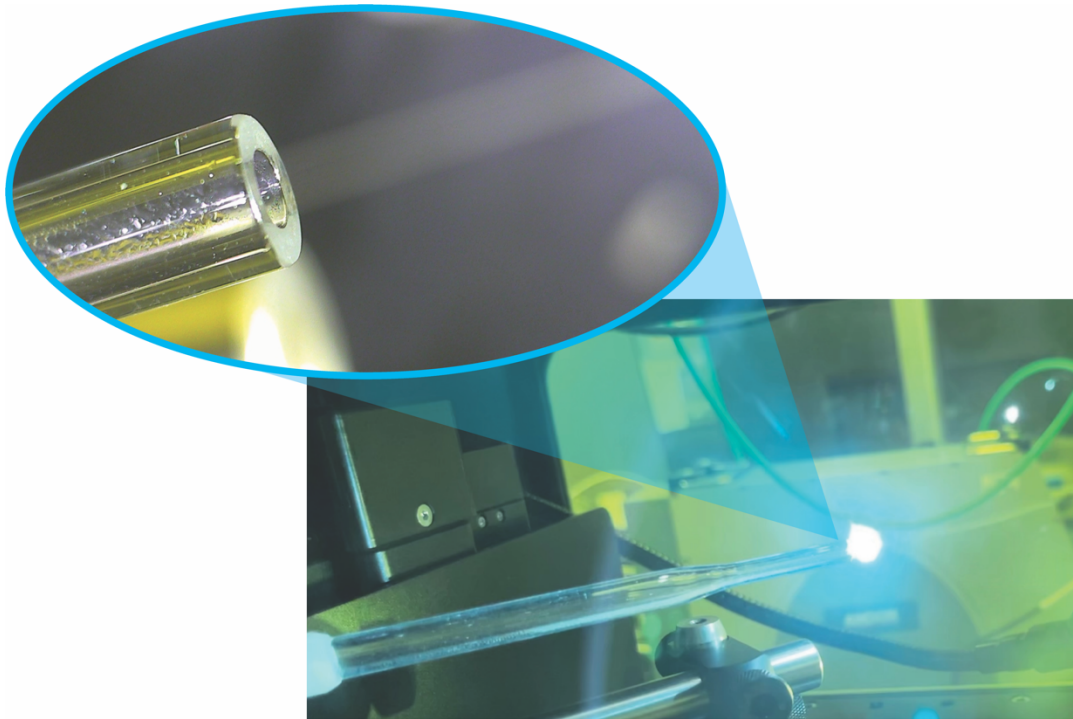


Figure 2. LIBS plasma being formed at the tip of the injector exit. The fine aerosol stream is shown in the cutaway image.

3. RESULTS AND DISCUSSION

3.1 MEASUREMENTS ON FILTER SUBSTRATES

Performing LIBS directly on liquids can be difficult because of plasma shockwave propagation effects. The shockwave that is generated with each laser pulse causes liquids to splash, risking the integrity of optical components. The subsequent wake leaves the liquid surface a variable distance from the optimal laser focal point. Although these issues can be counteracted through engineered sampling approaches, that is not the purpose of this study. Based on this knowledge, the initial H/D tests were performed by saturating glass fiber filters with varying aliquots of isotopic ratios and rastering the filter.

Based on the scan pattern selected, there were 64 shots per sample. The H emission line experiences significant Stark broadening, making its peak width stretch several nanometers. Single-shot emissions are typically very broad and subject to noise. To overcome this issue, several shots are accumulated such that the peak center can be better resolved. Using the gain feature on the ICCD, the emission was also intensified, which also increased the accuracy of measurement. Figure 3 demonstrates the variation found in single-shot spectra versus the averaged spectra. Although fewer shots can be averaged, it was found that averaging all 64 shots provided the best spectra for modeling.

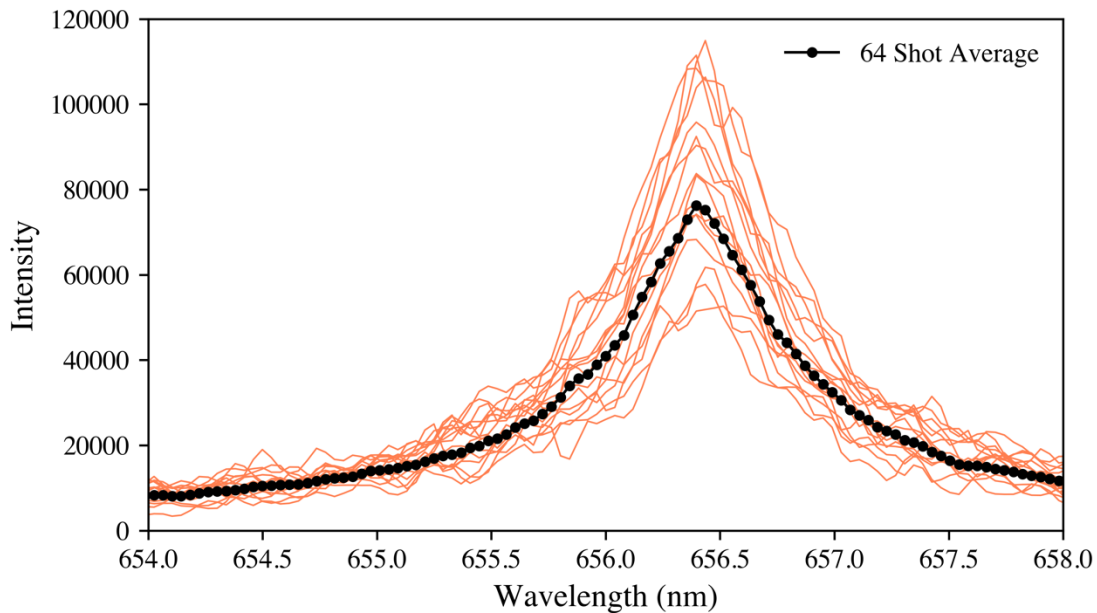


Figure 3. Single-shot spectra versus 64-shot average spectrum of 0% D₂O used to better resolve peak center.

A set of 11 filters were tested with D/H ratios ranging from 0% to 100% D₂O in steps of 10%. The peak shift as the isotopic ratio switches is shown in Figure 4(a). In addition to averaging the single-shot spectra, it was found that normalizing to the maximum intensity between 656 and 657 nm allowed for better compensation for any variation in laser energy. The peak center shifts from H to D, an apparent 158 pm to the blue, which is slightly less than the literature reported peak shift of approximately 179 pm.¹⁰ Additionally, a test sample was run containing 3,000 ppm Gd in D₂O to demonstrate that other species, such as the lanthanides, which are common fission products, could be monitored with the H isotopic ratio simultaneously. Figure 4(b) shows several Gd emission peaks in black, illustrating a very small fraction of the peaks available to monitor Gd in the test sample.

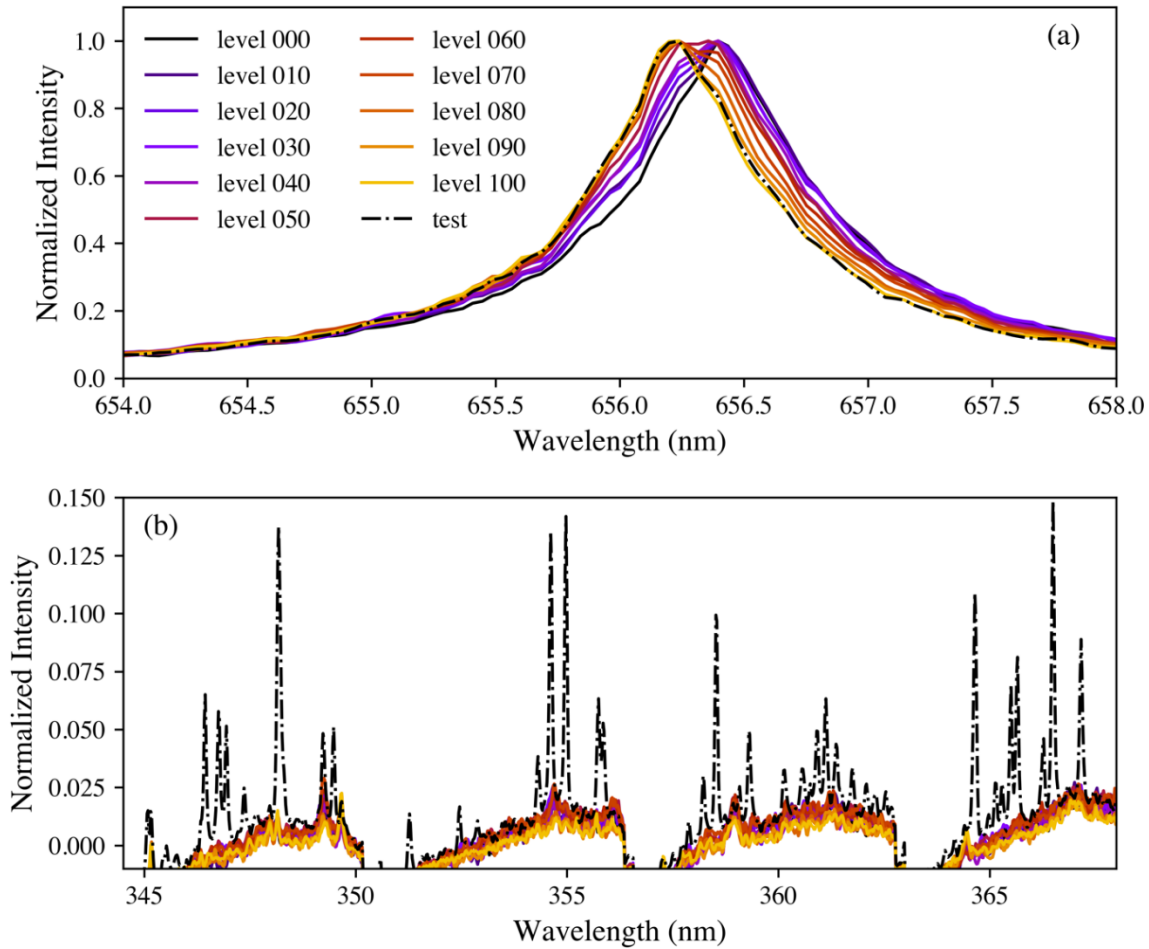


Figure 4. (a) Hydrogen emission line versus D/H ratio ranging from 0% to 100% D₂O and (b) the test sample shown with the dashed black line consists of 3,000 ppm Gd in 100% D₂O. The next step was to construct a regression model to quantify the isotope ratios of these samples. For this step, two multivariate methods—principal component regression (PCR) and partial least squares regression (PLSR)—were evaluated because these methods were better suited to deal with the convoluted D and H LIBS emissions. PCR is performed by doing a principal component analysis of the spectra, which involves iteratively solving for orthogonal principal components (PCs), which explain the most signal variance. These PCs are then used to transform a large-dimensional data set into a far smaller dimension (samples × PCs). PCR takes this transformation one step further, and a linear regression of the reduced data set is performed to predict the dependent variable (e.g., isotope ratio, species concentration, etc.). PLSR is similar to PCR but differs in two ways: first, the transformation and regression are done in one step, and second, rather than solve for PCs, which explain the most signal variance, PLSR solves for latent variables, which explain the most covariance between the signal and dependent variables. The latter difference typically makes PLSR results the better predictions.

To evaluate model performance, cross validation was performed using a leave-one-out cross validation (LOOCV) approach. Here, the model is iteratively built, leaving one sample out at a time, and then, at each iteration, the sample left out is used to test the model. The residuals for each sample while they are left out are used to calculate the root mean square error of cross validation (RMSECV):

$RMSECV = \sqrt{\frac{\sum (y_i - \hat{y}_i)^2}{n}}$, # (1) where y_i is the known concentration value of the i th sample left out during the LOOCV iteration, \hat{y}_i is the model-predicted concentration, and n is the number of samples.

The optimal models were built after three preprocessing steps. First, the spectra were smoothed using a Savitzky–Golay filter with a first order polynomial and a five-point window. Next, each spectrum was baseline-adjusted by subtracting the average background levels near the H peak. Lastly, each spectrum was normalized to the maximum intensity between 650 and 665 nm. For the PCR model, a two-component transform was used to convert the H emission into PC scores. Then ordinary least squares regression was used to relate these scores to the ratio of H/D. Similarly, only two latent variables were needed for the PLSR model. The parity plots for the PCR and PLSR models are shown in Figure 5. The RMSECV values were determined to be 1.9% and 2.0% for PCR and PLSR, respectively. Visually, the difference in prediction is hardly noticeable, with the calibration and cross-validation predictions matching nearly perfectly. As a final test, the sample of 3,000 ppm Gd in D₂O was predicted by the PCR and PLSR models to contain 96.2% and 96.1% D₂O, respectively. This decrease in D₂O from 100% can be explained by exchange with H₂O in the air because the solutions were not maintained in an inert atmosphere.

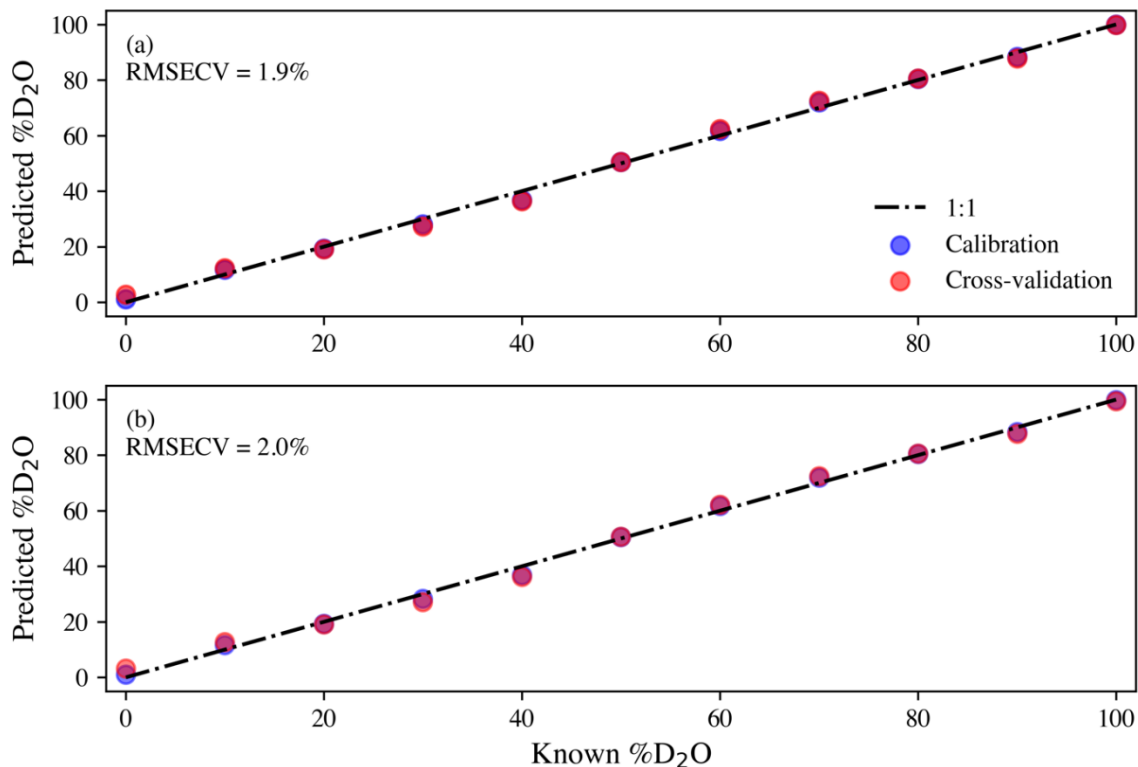


Figure 5. Parity plot comparing known versus predicted values of D₂O using (a) PCR and (b) PLSR. The closer the marker to the 1:1 line, the more accurate the prediction.

3.2 MEASUREMENTS ON AEROSOLS

Next, an aerosol system was tested as a better representation for monitoring an MSR core or off-gas system. For simplicity's sake, an aqueous aerosol system was constructed using off-the-shelf components previously used for inductively coupled plasma mass spectrometry sample introduction. Because of the natural variation in aerosol droplet size, a greater number of shots were accumulated to form an averaged spectrum for modeling. To facilitate the increased number of shots needed, the spectrometer configuration

was modified to only monitor 430–890 nm, which increased the maximum frame rate from 4.9 to 11 frames per second. This rate allowed the laser to be fired at 10 Hz. Spectra were saved in 100-shot accumulates, and samples were run for 1,000 shots (i.e., 100 s). Between each sample, air was pumped into the nebulizer for approximately 3 min to clear the system.

Optimal models were built using the averaged spectra of all 1,000 shots. Similar preprocessing steps were taken, but rather than normalizing to the H/D peak intensity, the spectra were normalized to the Ar 763 nm peak intensity. The Ar was used as the aerosol carrier gas that was flowed at a steady rate (1.7 L/min), which helped stabilize variance owing to laser energy fluctuation, plasma formation, and aerosol density. Again, only two PCs and latent variables were needed to appropriately describe the signal variance. The parity plots for the PCR and PLSR models are shown in Figure 6. The RMSECV values were determined to be 1.9% for both PCR and PLSR. This performance is equivalent to the filter calibration model, but these data were collected in a real-time monitoring configuration. As a final test of the aerosol models, a sample of the waste accumulated during the calibration was measured on the system. The D₂O level was predicted to be 79.9% and 80.0% by the PCR and PLSR models, respectively. These values make sense because the H₂O waste was drained after the first few calibration samples, leading to the subsequent collection having a higher D₂O level.

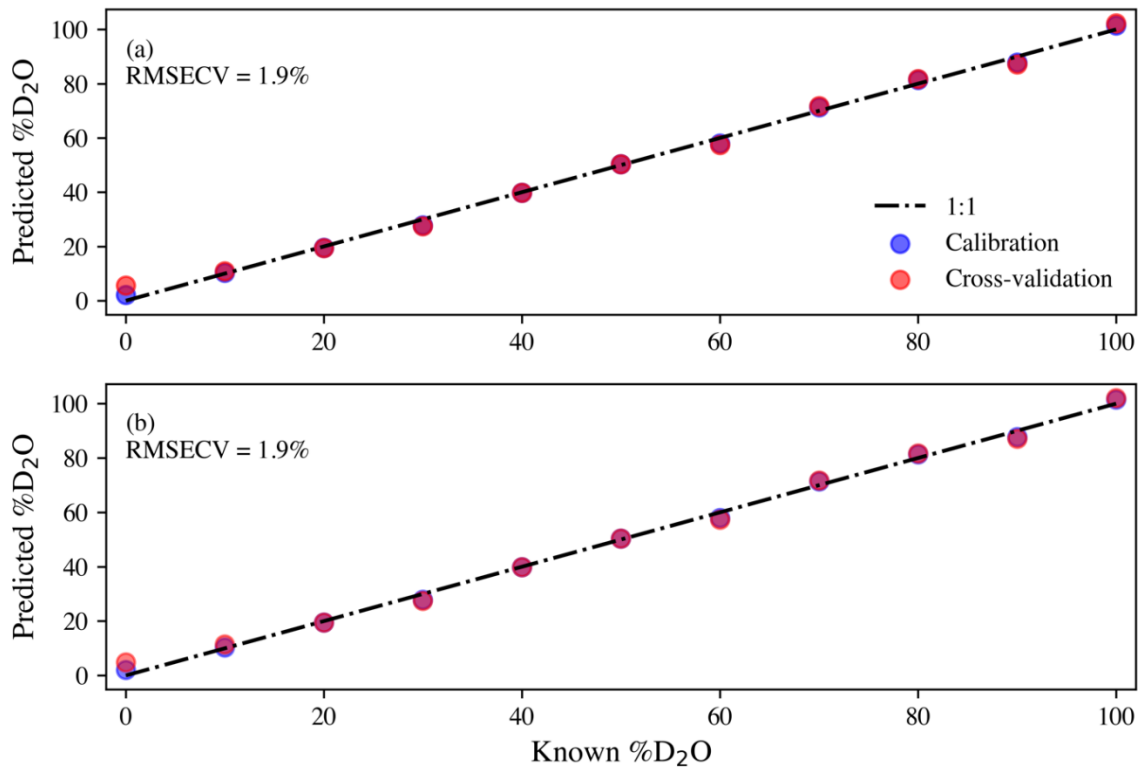


Figure 6. Parity plot comparing known versus predicted values of D₂O using (a) PCR and (b) PLSR. The closer the marker to the 1:1 line, the more accurate the prediction.

COMPARISON OF FILTER AND AEROSOL CALIBRATION MODELS

Because of the similar performance of both filter and aerosol models, the idea of calibration transfer between the two was of interest. For example, being able to calibrate a LIBS isotope model using the aliquots on filter approach would minimize time and experimental setup versus constructing an experimental setup analogous to a true application system. Additionally, the filter models required far less material than the aerosol models, which is of particular interest for future, more-expensive isotopes.

For this exercise, the filter models were reconstructed, and the aerosol samples were treated as a validation set. The same preprocessing used to build the filter models were applied to the aerosol spectra prior to prediction. The initial parity plot for the PCR model is shown in Figure 7. The same excellent fit of the calibration model to the 1:1 line can be seen, but the aerosol data consistently fall below the calibration model despite being baselined and normalized using the same process. Because the aerosol data appear to be parallel to the 1:1 line, it was theorized that a linear transformation was needed to compress the two systems into a singular compatible concentration. The differences in the calibration originate from the plasma formation differences between an aerosol and the ablation plasma of a solid filter.

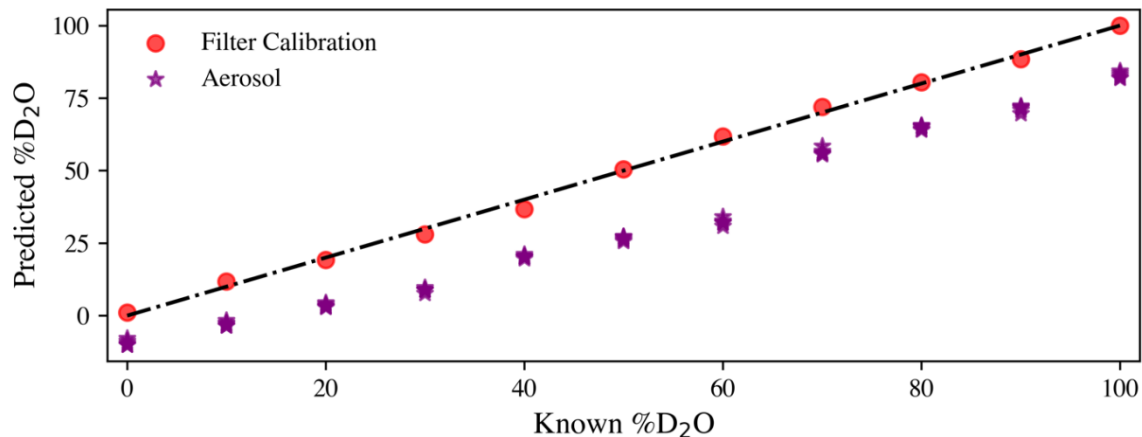


Figure 7. PCR model trained on filter data used to predict aerosol samples.

The spectra of both systems were normalized between 0 and 1, so no intensity transform was necessary. However, because the ablation and plasma mechanisms were different, an additional internal normalization was needed. Here, mean centering the spectra was applied as an additional preprocessing step. The results are shown in Figure 8. This additional step collapsed the two data sets onto one another and reduced the root mean square error of prediction (RMSEP) from 66% down to 6.3%. Although this RMSEP is greater than the 1,000-shot aerosol-trained model, it is insensitive to the replicates averaged. In other words, the RMSEP is consistent even if only 100 shots are used for the prediction. For comparison, if only 100 shots are used for the aerosol-trained model shown in Figure 6, the RMSECV is calculated to be 6.5%.

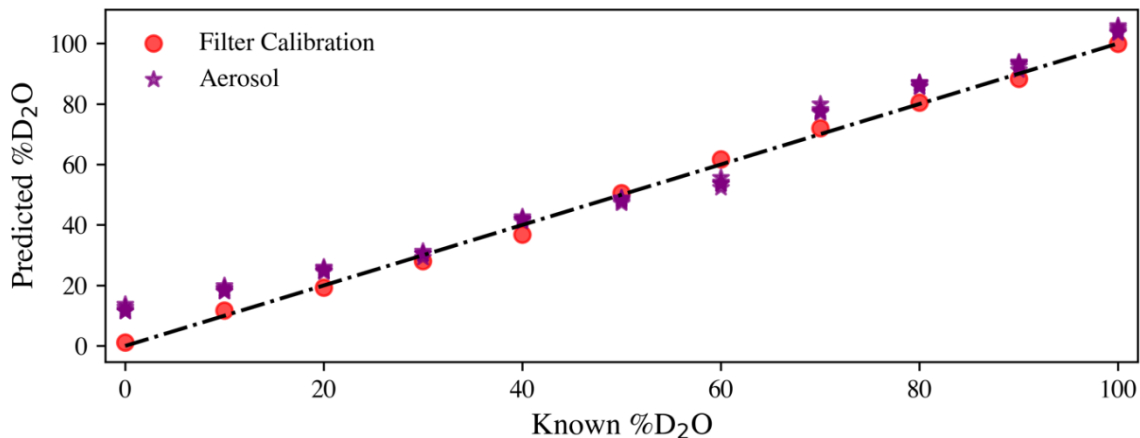


Figure 8. PCR model trained on filter data used to predict aerosol samples after the additional mean centering preprocessing step.

Although 6.3% error is greater than what would be ideal for an analytical measurement, this experiment does show that semiquantitative models for isotope shifts in LIBS can be built with alternative samples and then applied to process monitoring. This result is particularly appealing when the amount of material is compared. The filter tests required a total of 10 μ L per sample compared with 4 mL per sample for the aerosol tests, which is a difference of 99.8% in the volume of material consumed.

4. SUMMARY AND FUTURE WORK

This study demonstrates the expansion of Oak Ridge National Laboratory's LIBS capabilities to monitor isotopes by performing proof-of-principle H isotope ratios of aqueous aerosol systems and liquid droplets on filter paper. Both the models built using the filter samples and aerosol samples were capable of prediction errors as low as 1.9%. Furthermore, simple calibrations made using the filter approach may be extended to develop rapid, semiquantitative models for engineering-scale systems. This method was demonstrated by extrapolating the filter sample calibration to the aerosol samples with success. This approach may be vital for more cost-prohibitive isotopic systems.

Future work will focus on expanding the calibration library of isotopic systems available to be monitored at Oak Ridge National Laboratory. All subsequent isotopic shifts are far smaller as the elemental mass is increased. This smaller size necessitates higher-resolution spectrometers or the use of molecular signatures in the plasma, which experiences enhanced wavelength shifts. Additionally, a mobile LIBS system to be coupled with various molten salt systems across the lab complex is being developed in tandem to these efforts for deployable isotopic measurements.

5. ACKNOWLEDGMENTS

The authors would like to acknowledge Benjamin T. Manard for his assistance in setting up the aerosol components used for testing. This work was funded by the US Department of Energy's Office of Nuclear Energy, Advanced Reactor Development Program, Molten Salt Reactor Program.

6. REFERENCES

- (1) Andrews, H. B.; McFarlane, J.; Chapel, A. S.; Ezell, N. D. B.; Holcomb, D. E.; de Wet, D.; Greenwood, M. S.; Myhre, K. G.; Bryan, S. A.; Lines, A. Review of molten salt reactor off-gas management considerations. *Nucl Eng Des* **2021**, 385, 111529.
 - (2) Andrews, H.; Mcfarlane, J. *Characterization of surrogate molten salt reactor aerosol streams*; Oak Ridge National Laboratory, Oak Ridge, Tennessee (United States), 2021.
 - (3) Andrews, H. B.; McFarlane, J.; Myhre, K. G. Monitoring Noble Gases (Xe and Kr) and Aerosols (Cs and Rb) in a Molten Salt Reactor Surrogate Off-Gas Stream Using Laser-Induced Breakdown Spectroscopy (LIBS). *Applied Spectroscopy* **2022**, 00037028221088625.
 - (4) Andrews, H. B.; Myhre, K. G. Quantification of Lanthanides in a Molten Salt Reactor Surrogate Off-Gas Stream Using Laser-Induced Breakdown Spectroscopy. *Applied Spectroscopy* **2022**, 00037028211070323.
 - (5) Andrews, H. B.; Myhre, K. G.; McFarlane, J. Concept for an irradiation experiment to test a laser-induced breakdown spectroscopy off-gas sensor for molten salt systems. *Frontiers in Energy Research* **2023**, 10 (1).
 - (6) Andrews, H. B.; Thallapally, P. K.; Robinson, A. J. Monitoring Xenon Capture in a Metal Organic Framework Using Laser-Induced Breakdown Spectroscopy. *Micromachines* **2023**, 14 (1), 82.
 - (7) Felmy, H. M.; Clifford, A. J.; Medina, A. S.; Cox, R. M.; Wilson, J. M.; Lines, A. M.; Bryan, S. A. On-line monitoring of gas-phase molecular iodine using Raman and fluorescence spectroscopy paired with chemometric analysis. *Environmental Science & Technology* **2021**, 55 (6), 3898-3908.
 - (8) Medina, A. S.; Felmy, H. M.; Vitale-Sullivan, M. E.; Lackey, H. E.; Branch, S. D.; Bryan, S. A.; Lines, A. M. Iodine and Carbonate Species Monitoring in Molten NaOH–KOH Eutectic Scrubber via Dual-Phase In Situ Raman Spectroscopy. *ACS Omega* **2022**, 7 (44), 40456-40465.
 - (9) Harilal, S.; Brumfield, B.; LaHaye, N.; Hartig, K.; Phillips, M. Optical spectroscopy of laser-produced plasmas for standoff isotopic analysis. *Applied Physics Reviews* **2018**, 5 (2).
 - (10) Sarkar, A.; Mao, X. L.; Chan, G. C. Y.; Russo, R. E. Laser ablation molecular isotopic spectrometry of water for D-1(2)/H-1(1) ratio analysis. *Spectrochim Acta B* **2013**, 88, 46-53. DOI: 10.1016/j.sab.2013.08.002.
-